

## Complete Sequence and Genomic Analysis of Murine Gammaherpesvirus 68

HERBERT W. VIRGIN IV,<sup>1</sup> PHILIP LATREILLE,<sup>2</sup> PAMELA WAMSLEY,<sup>2</sup> KYMBERLIE HALLSWORTH,<sup>2</sup>  
KAREN E. WECK,<sup>1</sup> ALBERT J. DAL CANTO,<sup>1</sup> AND SAMUEL H. SPECK<sup>1\*</sup>

*Department of Pathology and Center for Immunology<sup>1</sup> and Genome Sequencing Center, Department of Genetics,<sup>2</sup> Washington University School of Medicine, St. Louis, Missouri 63110*

Received 19 February 1997/Accepted 16 April 1997

**Murine gammaherpesvirus 68 ( $\gamma$ HV68) infects mice, thus providing a tractable small-animal model for analysis of the acute and chronic pathogenesis of gammaherpesviruses. To facilitate molecular analysis of  $\gamma$ HV68 pathogenesis, we have sequenced the  $\gamma$ HV68 genome. The genome contains 118,237 bp of unique sequence flanked by multiple copies of a 1,213-bp terminal repeat. The GC content of the unique portion of the genome is 46%, while the GC content of the terminal repeat is 78%. The unique portion of the genome is estimated to encode at least 80 genes and is largely colinear with the genomes of Kaposi's sarcoma herpesvirus (KSHV; also known as human herpesvirus 8), herpesvirus saimiri (HVS), and Epstein-Barr virus (EBV). We detected 63 open reading frames (ORFs) homologous to HVS and KSHV ORFs and used the HVS/KSHV numbering system to designate these ORFs.  $\gamma$ HV68 shares with HVS and KSHV ORFs homologous to a complement regulatory protein (ORF 4), a D-type cyclin (ORF 72), and a G-protein-coupled receptor with close homology to the interleukin-8 receptor (ORF 74). One ORF (K3) was identified in  $\gamma$ HV68 as homologous to both ORFs K3 and K5 of KSHV and contains a domain found in a bovine herpesvirus 4 major immediate-early protein. We also detected 16 methionine-initiated ORFs predicted to encode proteins at least 100 amino acids in length that are unique to  $\gamma$ HV68 (ORFs M1 to 14). ORF M1 has striking homology to poxvirus serpins, while ORF M11 encodes a potential homolog of Bcl-2-like molecules encoded by other gammaherpesviruses (gene 16 of HVS and KSHV and the BHRF1 gene of EBV). In addition, clustered at the left end of the unique region are eight sequences with significant homology to bacterial tRNAs. The unique region of the genome contains two internal repeats: a 40-bp repeat located between bp 26778 and 28191 in the genome and a 100-bp repeat located between bp 98981 and 101170. Analysis of the  $\gamma$ HV68, HVS, EBV, and KSHV genomes demonstrated that each of these viruses have large colinear gene blocks interspersed by regions containing virus-specific ORFs. Interestingly, genes associated with EBV cell tropism, latency, and transformation are all contained within these regions encoding virus-specific genes. This finding suggests that pathogenesis-associated genes of gammaherpesviruses, including  $\gamma$ HV68, may be contained in similarly positioned genome regions. The availability of the  $\gamma$ HV68 genomic sequence will facilitate analysis of critical issues in gammaherpesvirus biology via integration of molecular and pathogenetic studies in a small-animal model.**

Gammaherpesviruses are characterized biologically by their association with tumors in immunosuppressed hosts. The prototypic gamma-2 herpesvirus, herpesvirus saimiri (HVS), causes lymphomas in some primates and rabbits and can transform T lymphocytes (32, 37, 46, 50). Epstein-Barr virus (EBV) is associated with lymphomas and nasopharyngeal carcinoma in humans (39, 60), and Kaposi's sarcoma herpesvirus (KSHV) is associated with Kaposi's sarcoma, body cavity-based lymphomas, and Castleman's disease in humans (12, 15, 20, 34, 40, 49, 63). Because EBV and KSHV have been found to be species specific, the only effective animal models for analysis of gammaherpesvirus pathogenesis have been HVS infection of primates or rabbits and EBV infection of marmosets. To help elucidate the pathogenesis of acute and chronic gammaherpesvirus infection, a mouse model of gammaherpesvirus infection has recently been developed.

Murine gammaherpesvirus 68 ( $\gamma$ HV68; also referred to as MHV68) is a natural pathogen of wild murid rodents (7), capable of infecting both outbred and inbred mice (8, 48, 58,

67). Viral genome structure and limited sequence analysis have indicated that  $\gamma$ HV68 is related to primate gammaherpesviruses (24, 25, 55, 64, 65).  $\gamma$ HV68 infects multiple organs of inbred mice and can establish a latent or persistent infection in the spleen (8, 58, 67, 68, 76). Both CD4 and CD8 T cells are important for control of  $\gamma$ HV68 infection (10, 26, 76), with persistent rather than latent infection seen in CD8-deficient mice (76) and progressive infection seen in CD4-deficient mice (10). One study implicated B lymphocytes as a potential reservoir of persistent and/or latent virus in infected mouse spleens (68). In addition, a B-lymphoma cell line chronically infected with  $\gamma$ HV68 has been isolated from an infected mouse (73). However, the issue of the cellular reservoir for latent virus remains unclear since subsequent analyses has demonstrated efficient establishment of latency in mice lacking mature B cells (76) and persistence of  $\gamma$ HV68 DNA in lungs of B-cell-deficient mice (74), raising the possibility that there are multiple or alternate sites of  $\gamma$ HV68 latency. In one study, a significant portion of mice infected with  $\gamma$ HV68 developed lymphoproliferative disorders, and treatment with cyclosporin A increased the frequency of lymphoproliferative disease (66). These initial studies strongly suggest that  $\gamma$ HV68 is biologically similar to primate gammaherpesviruses. To establish a molecular basis for analysis of  $\gamma$ HV68 pathogenesis, we have sequenced the  $\gamma$ HV68 genome.

\* Corresponding author. Mailing address: Department of Pathology, Box 8118, Washington University School of Medicine, 660 S. Euclid Ave., St. Louis, MO 63110. Phone: (314) 362-0367. Fax: (314) 362-4096. E-mail: speck@pathology.wustl.edu.

## MATERIALS AND METHODS

**Virus isolation and assay.**  $\gamma$ HV68 was kindly provided by Peter Doherty (St. Jude's Hospital, Memphis, Tenn.). We cloned  $\gamma$ HV68 by limiting dilution twice and designated the isolate that we sequenced the  $\gamma$ HV68 WUMS (for Washington University School of Medicine) clone. This strain has been submitted to the American type culture collection. NIH 3T12 and mouse embryonic fibroblasts (MEFs) were maintained in Dulbecco's modified Eagle medium supplemented with 10% fetal calf serum, penicillin (100 U/ml), streptomycin (100 mg/ml), and 2 mM L-glutamine. MEFs were obtained as previously described (57). Plaque assays were performed on NIH 3T12 cells as previously described (76).

**Preparation of viral DNA.** Virus stocks for preparation of DNA were grown (multiplicity of infection of 1.0) in mouse NIH 3T12 fibroblasts. Virus was harvested from the culture supernatants 4 to 6 days postinfection (three T225 tissue culture flasks of NIH 3T12 fibroblasts were infected for DNA preparation). Cellular debris was removed from the culture supernatant by centrifugation at  $1,000 \times g$  for 20 min. Virus was pelleted by centrifugation at  $14,000 \times g$  for 2 h at 4°C. The virus pellet was gently washed three times with 5 ml of cold phosphate-buffered saline and then resuspended in 1 ml of DNase I digestion buffer (50 mM Tris [pH 7.5], 10 mM MgCl<sub>2</sub>, 50  $\mu$ g of bovine serum albumin per ml) and adjusted to a final volume of 2 ml with DNase I digestion buffer. DNase I (Worthington) was added to a final concentration of 1.4  $\mu$ g/ml and allowed to digest for 30 min at 37°C. The virus suspension was then layered onto a 20% sucrose cushion (20% sucrose, 20 mM Tris [pH 7.5], 150 mM NaCl, 1 mM EDTA) in TLS55 tubes (Beckman), and virus was pelleted at  $111,000 \times g$  for 1 h at room temperature in a TLS55 swinging-bucket rotor (Beckman). The viral pellet was resuspended in 3 ml of 10 mM Tris (pH 8.0)–1 mM EDTA, and 3 ml of 2 $\times$  lysis buffer (40 mM Tris [pH 7.5], 200 mM NaCl, 20 mM EDTA, 2% Sarkosyl, 0.5% sodium dodecyl sulfate) was added. Proteinase K was added to a final concentration of 333  $\mu$ g/ml, and the reaction mixture was incubated at 37°C overnight. The reaction mixture was then gently extracted with an equal volume phenol-chloroform (1:1, vol/vol) by rocking for 30 min, followed by centrifugation at  $3,000 \times g$  for 10 min. The aqueous phase was reextracted with an equal volume of chloroform by rocking for 30 min and centrifuged to separate the phases. The aqueous phase was recovered, and viral DNA was precipitated by addition of sodium acetate to a final concentration of 0.3 M and 2 volumes of ethanol. DNA was analyzed by pulsed-field gel electrophoresis and shown to migrate as a single large band.

To ensure that the DNA isolated contained all sequences required for  $\gamma$ HV68 replication, we transfected the full-length DNA into NIH 3T12 fibroblast cells by the calcium phosphate-dimethyl sulfoxide shock method (11). In two independent experiments, transfection of the purified viral DNA generated infectious  $\gamma$ HV68 (not shown). As a control, we showed that no infectious virus was present in the viral DNA preparation by the absence of viral cytopathic effect in MEF cultures to which viral DNA was added (without transfection). The MEF assay used is 10-fold more sensitive for detecting infectious  $\gamma$ HV68 than the plaque assay on NIH 3T12 fibroblasts (76).

**DNA sequence generation.** Purified viral DNA was sheared by sonication; ends were blunted with mung bean nuclease, size fractionated by gel electrophoresis, purified, ligated into M13 vector restricted with *Sma*I, and phosphatase treated as described elsewhere (77). Single-stranded DNA from M13 subclones was prepared by using the modified high-throughput ThermoMAX procedure (45). The single-stranded DNA was sequenced by using a cycling protocol (30) with fluorescent dye-labeled ET primers (35) and Thermosequase (Amersham Inc., Arlington Heights, Ill.). Reaction products were analyzed on ABI 373A (stretch modified) and 377 automated sequencers (77). DNA sequence data was processed by using the OTTO script (33a). Base calling and sequence assembly were performed by using PHRED and CONSED (32a) followed by XGAP (19). The program FINISH (45a) was used to analyze the initial assembly in order to generate a list of specific reads necessary to obtain complementary strand coverage, close gaps, and resolve ambiguities. All final reads necessary to complete the genome sequence were performed and entered into the database (77). The entire sequence was represented by coverage either on both strands or with orthologous chemistries to resolve any ambiguities. The sequence data for the two tandem repeats were derived as discussed elsewhere in this report. Sequence assemblies were verified by constructing *Eco*RI, *Hind*III, and *Bam*HI maps of the assembled sequence and comparing them with the published maps of the  $\gamma$ HV68 genome (25).

To obtain sequences within the 100-bp internal repeat, the *Hind*III (95,678 bp)-*Eco*RI (102,216 bp) fragment of the genome containing the repeat was cloned into BlueScript KS+ (Stratagene). This clone was digested with *Nhe*I (cuts at 101,676 bp in the viral genome) and *Pst*I (cuts within the polylinker of BlueScript). Nested deletions were generated by using an exonuclease III, S1 nuclease deletion kit (Erase-a-Base kit; Promega) according to the manufacturer's protocol. Appropriate size deletions were sequenced as described above in the presence of 7.5% dimethyl sulfoxide to help resolve sequence compressions.

**DNA sequence analysis and analysis of putative gene products.** Repeated sequences were identified within the finished sequences, using TANDEM and INVERTED (22a). Initial analysis of the coding content of the genome was performed by using ACEDB (22b). For analysis of individual open reading frames (ORFs), the genome was downloaded into VECTOR NTI version 4.0 Deluxe (Informax Inc., Gaithersburg, Md.). ORFs were translated in VECTOR

NTI and downloaded to the National Center for Biotechnology Information (NCBI) BLAST server for analysis by BLASTP. Regions of the  $\gamma$ HV68 nucleotide sequence were downloaded for analysis by BLASTN and BLASTX. Unless otherwise specified, default settings (including filters) were used for BLAST searches. Alignments between  $\gamma$ HV68 ORFs and genes in other viruses, or host proteins, were analyzed by using the DNASTAR suite of programs (DNASTAR Inc., Madison Wis.). Alignments were performed with MegAlign, using the PAM250 residue weight table. Identities were determined from the PAM250 MegAlign alignments and are reported as the percentage of amino acids in a gene identical to the  $\gamma$ HV68 sequence divided by the number of amino acids in the  $\gamma$ HV68 ORF. Phylogenetic analyses were performed with MegAlign and the PAM250 weight table. Analysis of potential tRNA genes present in the  $\gamma$ HV68 genome was carried out by using the tRNAscan-SE program (43a), which uses a modified, optimized version of tRNAscan version 1.3 (28), coupled with a new implementation of a multistep weight matrix algorithm for identification of eukaryotic tRNA promoter regions (54) as well as the RNA covariance analysis package Cove version 2.4.2 (23).

**Assignment of ORFs and nomenclature.** We initially scanned the viral genome for methionine-initiated ORFs encoding putative proteins at least 100 amino acids in length. Each of these ORFs was searched versus the nonredundant NCBI database, using the BLASTP algorithm and default settings, between January 1 and January 30, 1997. Viral and/or host homologs of all  $\gamma$ HV68 ORFs with significant scores were downloaded for alignment and analysis. Subsequently, a list of genes in HVS that were not found in the  $\gamma$ HV68 sequence by using the initial criteria was compiled. The presence of these genes was reevaluated by searching regions of the  $\gamma$ HV68 genome (assuming the HVS gene order) and analyzing all methionine-initiated ORFs encoding proteins at least 50 to 60 amino acids in length, using BLASTP. In addition, these regions of the  $\gamma$ HV68 genome were screened by using BLASTX to assess the presence of short ORFs with homology to HVS genes not identified by the previous searches. These approaches were successful in identifying several homologs of HVS ORFs that were missed on the initial search due to their short length. ORFs with homology to previously described gammaherpesvirus genes and ORFs were named for their HVS and KSHV homologs. After assignment of ORFs with known viral homologs, we examined the remaining 100 amino acid ORFs, using the following criteria. We evaluated whether the nucleotide sequences encoding these ORFs overlapped by more than 30% the nucleotide sequences encoding ORFs with homology to HVS, KSHV, and/or EBV genes. If ORFs overlapped known ORFs by less than 30%, we concluded that they might represent  $\gamma$ HV68-specific ORFs and designated them M ORFs (for murine  $\gamma$ HV68 putative ORFs). ORFs that overlapped more extensively with ORFs encoding homologs of known gammaherpesvirus proteins are not reported. This method of analysis does not address the possibility of gene products smaller than 100 amino acids in length or those that arise from splicing small ORFs and thus is most likely a conservative estimate of the number of genes encoded by  $\gamma$ HV68.

**GenBank accession number.** The complete sequence of the unique region of the  $\gamma$ HV68 genome has been deposited in the NCBI database. The accession number is GAMMAHV U97553.

## RESULTS AND DISCUSSION

**Primary structure of the  $\gamma$ HV68 genome.** Sequences from 2,336 random M13 bacteriophage recombinants (and additional clones described below) were assembled into a contiguous sequence (contig) representing the entire unique region of the  $\gamma$ HV68 genome linked to a copy of the 1,213-bp terminal repeat at the right end of the unique sequence (Fig. 1; total length of the contig is 119,450 bp). The linear organization of the genome was deduced from the previous characterization of the  $\gamma$ HV68 genome (25), which demonstrated the presence of multiple 1.2-kb direct repeats (terminal repeats) flanking the unique region of the genome. Based on the orientation of the HVS and KSHV genomes, the first base pair of unique sequence on the left end of the genome adjacent to the terminal repeat was assigned nucleotide position 1. The length of the unique region of the genome was determined from the sequence to be 118,237 bp, in close agreement with the 118 kb predicted by physical mapping of the  $\gamma$ HV68 genome (25). The previously deduced *Bam*HI, *Hind*III, and *Eco*RI restriction endonuclease maps of the genome matched closely those predicted from the nucleotide sequence (Fig. 1A and reference 25). Exceptions were several small fragments not previously observed: (i) a 209-bp *Hind*III fragment (*Hind*III a) between the *Hind*III H and Y fragments, (ii) a 280-bp *Bam*HI fragment (*Bam*HI U) between the *Bam*HI K and A2 fragments, and (iii)

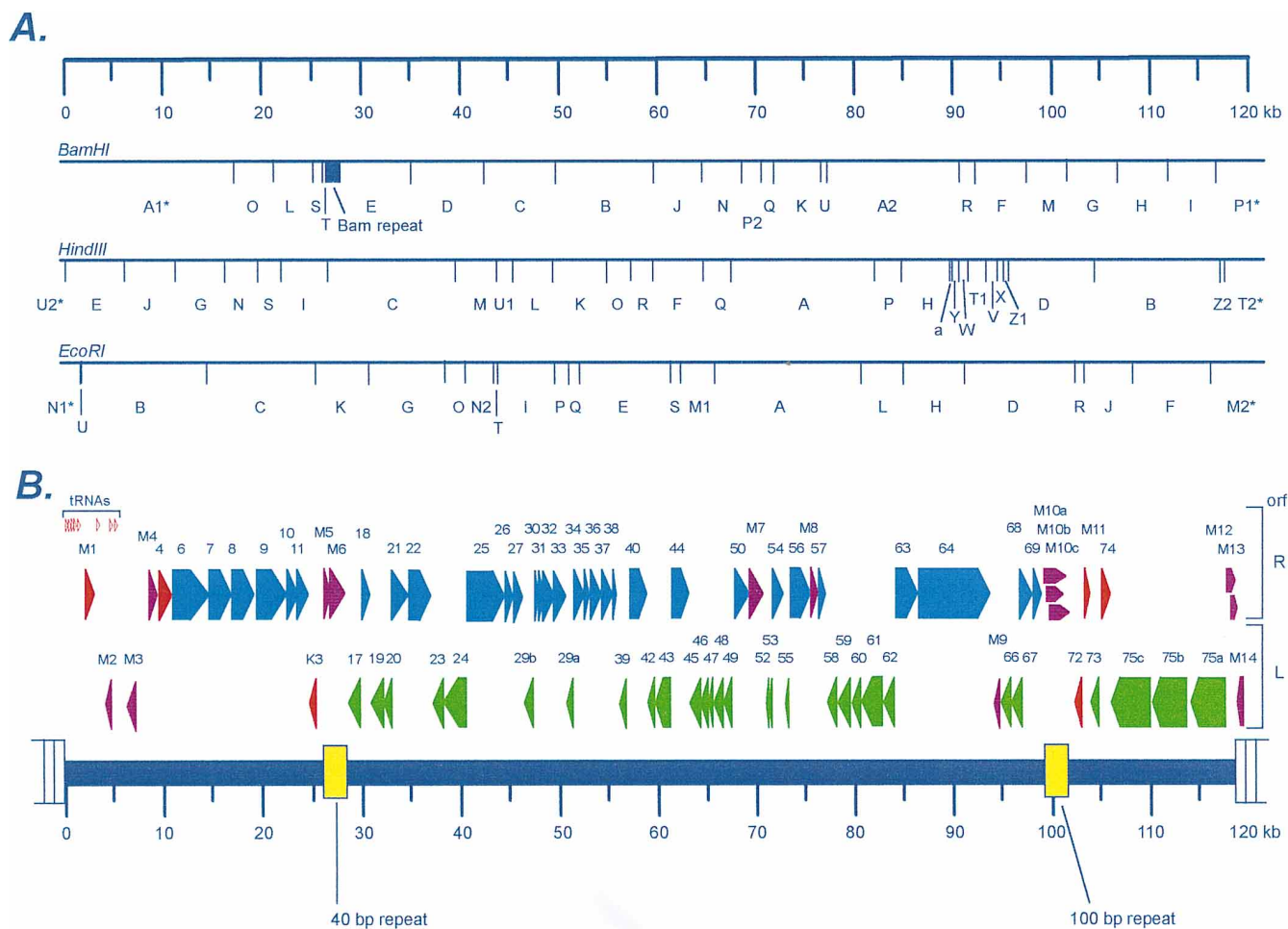


FIG. 1. Organization and ORF analysis of the  $\gamma$ HV68 genome. (A) Predicted *Bam*HI, *Eco*RI, and *Hind*III restriction endonuclease cleavage maps of the  $\gamma$ HV68 genome based on the complete nucleic acid sequence. With the exception of several small fragments (*Bam*HI U, *Hind*III a, and *Eco*RI U), the predicted maps closely match the published analysis of Efstathiou et al. (25). Asterisks indicate fragments at the ends of the genome map which have an undefined size due to the presence of a variable number of terminal repeats. (B) ORFs and tRNA-like genes present in the  $\gamma$ HV68 genome. The  $\gamma$ HV68 genome is composed of a 118,237-bp unique region (shown as the thick blue line) flanked by multiple copies of a 1,213-bp terminal repeat (depicted as open rectangles at the ends of the genome). In addition, there are two internal repeats within the unique region, which are shown in yellow. The criteria for selecting candidate ORFs are described in the text. Those ORFs with substantial homology to genes present in the HVS and KSHV genomes were assigned the corresponding HVS/KSHV gene number. Rightward ORFs of HVS homologs are depicted in blue, while leftward ORFs of HVS homologs are depicted in green (with the exception of those which are homologs of known cellular genes).  $\gamma$ HV68 ORFs with no obvious homology to any other gammaherpesvirus genes were designated M ORFs (M1 to M14).  $\gamma$ HV68 ORFs which are homologs of known cellular genes or of genes in viruses other than HVS, KSHV, and EBV are depicted in red. Those M ORFs which do not exhibit significant homology to any known cellular or viral gene products are indicated in purple. Also shown clustered near the left end of the unique region are eight potential tRNA-like genes (see Table 2 for details).

a 53-bp *Eco*RI fragment (*Eco*RI U) between the *Eco*RI NI\* and B fragments (Fig. 1A).

The unique region of the genome is ca. 46% G+C, while the terminal repeat is 77.6% G+C. This is comparable to the 53.5% G+C content of the unique region and 84.5% G+C content of the terminal repeats of KSHV (61). Similarly, the G+C content of the unique region of equine herpesvirus 2 (EHV2) is 58% (70). However, the G+C contents of the unique region of both  $\gamma$ HV68 and KSHV are significantly higher than the 34.5% G+C content of the unique region of HVS (3). Similar to both  $\gamma$ HV68 and KSHV, the terminal repeat of HVS is very G+C rich (70.8%) (3).

**Analysis of putative ORFs in  $\gamma$ HV68.** Computer sequence analysis predicted the presence of 80 ORFs in the  $\gamma$ HV68 genome (Fig. 1 and Table 1). The basis for assigning ORFs was (i) ATG-initiated ORFs predicted to encode a minimum of 100 amino acids (exceptions were made in cases where a known or predicted gene product is encoded by another gam-

maherpesvirus), (ii) significant sequence homology to other known viral or cellular genes, and/or (iii) less than a 30% overlap with ORFs defined by the first two criteria. These predicted ORFs are shown relative to the  $\gamma$ HV68 map in Fig. 1. Table 1 summarizes their locations in the genome, predicted polypeptide sizes, and percent sequence identities to KSHV, HVS, and EBV gene products. Putative gene products with homology to HVS gene products were assigned the HVS/KSHV gene number (i.e., ORF 4 corresponds to HVS gene 4), while  $\gamma$ HV68 ORF products which are not obvious homologs of other gammaherpesvirus genes were designated M ORFs (e.g., M1 [Fig. 1 and Table 1]). It is likely that this ORF analysis reflects a conservative estimate of the genes encoded by  $\gamma$ HV68 since numerous small ORFs which did not meet these criteria are not represented in Table 1 and Fig. 1. Furthermore, this analysis would not detect spliced genes containing either short (<300 bp) or non-ATG-initiated ORFs.

Of the 80 ORFs identified in the  $\gamma$ HV68 genome, 63 are

TABLE 1. Putative  $\gamma$ HV68 gene products and homologs present in other gammaherpesviruses

Name	Genome location (bp)	Coding strand	Size (amino acids)				EBV name	% Identity to $\gamma$ HV68			Possible function <sup>a</sup>
			$\gamma$ HV68	KSHV	HVS	EBV		KSHV	HVS	EBV	
M1	2023-3282	R	420								Serpin
M2	4031-4627	L	199								
M3	6060-7277	L	406								
M4	8409-9785	R	459								
ORF 4	9873-11036	R	388	550	360			27.8	24.5		Complement regulatory protein
ORF 6	11215-14523	R	1,103	1,133	1,128	1,128	BALF2	40.3	42.2	39.6	Single-stranded DNA binding protein
ORF 7	14526-16481	R	652	695	679	685	BALF3	34.0	34.0	33.3	Transport protein
ORF 8	16505-19051	R	849	845	808	857	BALF4	51.1	45.6	38.2	Glycoprotein B
ORF 9	19217-22297	R	1,027	1,012	1,009	1,015	BALF5	55.8	55.1	49.2	DNA polymerase
ORF 10	22269-23522	R	418	418	407	422	RajiLF1	19.9	18.2	12.4	
ORF 11	23488-24651	R	388	407	405	429	RajiLF2	18.6	19.8	20.4	
K3	24733-25335	L	201	333				23.4			BHV4 IE1 homolog
M5	26178-26672	R	165								
M6	26554-28308	R	585								
ORF 17	28326-29957	L	544	553	475	605	BVRF3	32.7	28.3	28.3	Capsid protein
ORF 18 <sup>b</sup>	29917-30768	R	284	257	256	247	BVLF1.5	37.7	37.3	29.6	
ORF 19	30726-32273	L	516	549	543	570	BVRF1	36.2	38.8	34.5	Tegument protein
ORF 20	32119-32880	L	254	320	303	248	BXRF1	28.7	27.6	34.6	
ORF 21	32879-34810	R	644	580	527	607	BXLF1	19.6	19.9	20.8	Thymidine kinase
ORF 22	34833-37022	R	730	730	717	706	BXLF2	26.7	26.2	19.6	Glycoprotein H
ORF 23	37025-38167	L	381	404	253	425	BTRF1	25.2	13.6	21.5	
ORF 24	38103-40253	L	717	752	731	618	BcRF1	38.9	40.7	25.5	
ORF 25	40263-44381	R	1,373	1,376	1,371	1,381	BcLF1	56.8	57.2	52.4	Major capsid protein
ORF 26	44423-45319	R	299	305	304	301	BDLF1	42.1	38.8	33.8	Capsid protein
ORF 27	45329-46090	R	254	290	280	420	BDLF2	14.6	17.7	16.5	
ORF 29b	46395-47438	L	348	351	380	387	BDRF1	49.7	49.4	48.0	Packaging protein
ORF 30	47507-47746	R	80	77	75			27.5	32.5		
ORF 31	47710-48309	R	200	224	208	225	BDLF4	31.0	35.5	26.5	
ORF 32	48294-49625	R	444	454	441	507	BGLF1	20.7	23.0	20.5	
ORF 33	49588-50568	R	327	312	330	336	BGLF2	29.7	32.9	31.5	
ORF 29a	50549-51466	L	306	312	303	325	BGRF1	39.8	41.4	36.5	Packaging protein
ORF 34	51465-52460	R	332	327	316	332	BGLF3	28.0	31.6	27.7	
ORF 35	52423-52878	R	152	150	150	153	BGLF3.5	28.3	22.4	26.3	
ORF 36	52847-54157	R	437	444	431	455	BGLF4	23.8	18.8	24.3	Kinase
ORF 37	54129-55586	R	486	486	483	470	BGLF5	43.8	45.3	37.4	Alkaline exonuclease
ORF 38	55544-55768	R	75	61	66	75	BBLF1	20.0	20.0	24.0	Myristylated tegument protein
ORF 39	55802-56950	L	383	399	366	405	BBRF3	46.5	44.1	39.4	Glycoprotein M
ORF 40	57046-58875	R	610	457	450	541	BBLF2	18.4	20.5	13.1	Helicase-primase
ORF 42	58876-59634	L	253	278	265	278	BBRF2	33.6	35.6	28.9	
ORF 43	59634-61334	L	567	605	563	613	BBRF1	47.1	49.4	43.6	Capsid protein
ORF 44	61303-63630	R	776	788	781	809	BBLF4	54.8	53.1	47.0	Helicase-primase
ORF 45	63655-64272	L	206	407	257	214	BKRF4	33.0	13.1	13.6	
ORF 46	64275-65021	L	249	255	252	255	BKRF3	54.6	53.4	55.4	Uracil DNA glycosylase
ORF 47	65027-65545	L	173	167	141	137	BKRF2	20.2	15.6	13.9	Glycoprotein L
ORF 48	65584-66582	L	333	402	797	537	BKRF2	14.4	17.4	12.3	
ORF 49	66741-67643	L	301	302	303	310	BRRF1	14.6	16.0	12.6	
ORF 50	67907-69373	R	489	631	535	605	BRLF1	16.4	26.6	13.1	Transcriptional activator
M7	69466-70914	R	483								Glycoprotein 150
ORF 52	70960-71364	L	135	131	115	162	BLRF2	28.2	27.4	40.0	
ORF 53	71447-71701	L	85	110	90	102	BLRF1	30.6	30.6	27.1	
ORF 54	71806-72702	R	299	318	287	278	BLLF3	28.1	24.7	25.1	dUTPase
ORF 55	72744-73313	L	190	227	200	218	BSRF1	41.6	40.5	47.9	
ORF 56	73289-75793	R	835	843	835	874	BSLF1	35.3	35.7	30.5	DNA replication protein
M8	76015-76485	R	157								
ORF 57	76662-77159	R	166	275	416	438	BMLF1	21.7	25.3	22.3	Immediate-early protein
ORF 58	77214-78254	L	347	357	357	357	BMRF2	20.5	22.2	19.3	
ORF 59	78258-79439	L	394	396	368	404	BMRF1	32.7	26.1	24.4	DNA replication protein
ORF 60	79565-80479	L	305	305	305	302	BaRF1	61.3	62.3	56.1	Ribonucleotide reductase, small
ORF 61	80517-82865	L	783	792	767	826	BORF2	44.6	45.6	39.8	Ribonucleotide reductase, large
ORF 62	82871-84010	L	380	331	330	364	BORF1	25.0	20.2	22.1	Assembly/DNA maturation
ORF 63	83751-86564	R	938	928	899	1,239	BOLF1	21.6	21.0	17.3	Tegument protein
ORF 64	86567-93937	R	2,457	2,635	2,469	3,149	BPLF1	25.6	23.6	20.1	Tegument protein
M9	93962-94519	L	186								
ORF 66	94515-95741	L	409	429	435	591	BFRF2	31.1	29.6	23.0	
ORF 67	95738-96415	L	226	271	235	336	BFRF1	40.3	39.4	36.7	Tegument protein
ORF 68	96673-98052	R	460	545	436	525	BFLF1	31.7	29.1	29.3	Glycoprotein
ORF 69	98061-98936	R	292	225	261	318	BFLF2	33.9	35.6	32.9	
M10a	98903-101224	R	774								
M10b	99087-101204	R	706								
M10c	99187-101367	R	727								

Continued on following page

TABLE 1—Continued

Name	Genome location (bp)	Coding strand	Size (amino acids)				EBV name	% Identity to $\gamma$ HV68			Possible function <sup>a</sup>
			$\gamma$ HV68	KSHV	HVS	EBV		KSHV	HVS	EBV	
ORF 72	102426–103181	L	252	257	254			25.0	21.0		Cyclin D homolog
M11	103418–103930	R	171	175	160	191	BHRF1	11.7	11.7	24.8	Bcl-2 homolog (gene 16?)
ORF 73	103927–104868	L	314	1,162	407			24.2	7.3		Immediate-early protein
ORF 74	105057–106067	R	337	342	321			23.1	22.8		GCR (IL-8 receptor homolog?)
ORF 75c	106070–109999	L	1,310	1,296	1,299	1,318	BNRF1	24.7	23.4	22.4	Tegument protein/FGARAT <sup>c</sup>
ORF 75b	110077–113901	L	1,275	1,296	1,299	1,318	BNRF1	22.6	22.5	22.3	Tegument protein/FGARAT
ORF 75a	114032–117904	L	1,291	1,296	1,299	1,319	BNRF1	22.7	22.5	22.2	Tegument protein/FGARAT
M12	117992–118681	R	212								
M13	118149–118784	R	230								
M14	118808–119125	L	106								

<sup>a</sup> Functions of individual viral genes were based on information summarized in references 3, 6, 61, and 70.

<sup>b</sup> There is significant homology between  $\gamma$ HV68, KSHV, and HVS ORF 18 sequences and two overlapping reading frames in the EBV genome. The putative BVLF1.5 gene joins these ORFs based on elimination of a hypothetical frameshift as previously suggested (3).

<sup>c</sup> FGARAT, *N*-formylglycinamide ribotide amidotransferase.

homologs of HVS genes, all of which are also present in the KSHV genome and many of which are present in the EBV genome (Table 1). One ORF, K3, appears to be present in the KSHV and  $\gamma$ HV68 genomes but not in the HVS or EBV genome. The overall identity of  $\gamma$ HV68 ORFs to their homologs in the other gammaherpesviruses indicates that  $\gamma$ HV68 is more closely related to HVS and KSHV than to EBV (Table 1). However, at the level of individual ORFs, there is considerable variability in the extent of homology, and there are several ORFs for which the putative  $\gamma$ HV68 ORF product is most closely related to the EBV gene product (see below). It should be noted that we assigned  $\gamma$ HV68 genes as homologs of other gammaherpesvirus genes only when BLASTP analyses identified regions of homology (see Materials and Methods). Thus, for example, the  $\gamma$ HV68 M9 ORF may be the homolog of HVS and KSHV ORF 65 and/or EBV BFRF3, but none of these gene products were sufficiently homologous to the putative  $\gamma$ HV68 M9 gene product to score in the BLASTP search.

There was generally good size conservation between  $\gamma$ HV68 ORFs and those in KSHV, HVS, and EBV (Table 1). One exception is ORF 57 of  $\gamma$ HV68, which is significantly shorter than the KSHV, HVS, and EBV homologs. On further analysis, we found that ORF 57 is open upstream of the ATG at position 76662, which was used to calculate the size of the putative ORF 57 protein (Table 1). A BLASTP search of the ORF upstream of position 76662 revealed significant homology to HVS gene 57. In addition, alignment of this upstream region demonstrated significant homology with portions of the HVS and KSHV gene 57 proteins and the EBV BMLF1 gene. This finding suggests that  $\gamma$ HV68 ORF 57 may be a spliced gene, with the ATG-initiated ORF in Table 1 present as the C-terminal portion of a longer ORF 57 product.

It is also notable that there are three copies of ORF 75, which encodes the enzyme *N*-formylglycinamide ribotide amidotransferase. Interestingly, HVS also contains an additional copy of this gene (ORF 3). However, the other characterized gammaherpesviruses appear to encode only a single copy of ORF 75. The significance of multiple copies of this gene in  $\gamma$ HV68 and HVS in the biology of these viruses is not readily apparent.

In general, the  $\gamma$ HV68 ORFs are very closely spaced on the genome (Fig. 1 and Table 1). The exception to this is near the left end of the unique region, where the presence of ORFs which meet the criteria described above is relatively sparse. As discussed below, this may be notable since among the gamma-herpesviruses, this region is very divergent and, in the cases of

EBV and HVS, is known to encode transformation-associated gene products (6, 21, 32, 37, 39, 47, 50). At the left end of the  $\gamma$ HV68 genome, five short (40- to 104-bp) sequences with significant homology to multiple (at least three different) bacterial tRNAs were detected by a BLASTN search of bp 1 to 10000 of the genome (Fig. 1). Additional sequences with some homology to a single bacterial tRNA were also found in this region. BLASTN searches of the remainder of the genome did not reveal any additional tRNA-like sequences. The first 10,000 bp of the genome was further evaluated by using the tRNAscan-SE program (see Materials and Methods), which predicted the presence of eight tRNA-like genes (Table 2). The role of these putative tRNA-like molecules in the  $\gamma$ HV68 life cycle is not clear, and it is possible that they do not function as tRNAs since five of the eight tRNA-like genes lack clear anticodons (Table 2). Interestingly, the putative tRNAs are encoded in a region positionally homologous to the region encoding the HVS U-RNAs (2, 3, 31, 50).

Three of the  $\gamma$ HV68-specific ORFs (M12, M13, and M14) are partially or entirely encoded within the terminal repeat (below). The significance of this remains to be determined, since the high G+C content of the terminal repeats may predict the presence of ORFs which are not actually transcribed. Similarly, three overlapping ORFs (M10a, M10b, and M10c) which are largely encoded within the 100-bp repeat were detected. These share a common repetitive sequence encoded by the 100-bp repeat but are predicted to contain unique carboxy termini. In addition, M10a is predicted to have a unique amino-terminal sequence (compared to ORFs M10b and M10c) since this ORF initiates 78 bp to the left of the 100-bp repeat. ORF M6 spans the 40-bp repeat and is predicted to have a repetitive amino acid sequence.

TABLE 2. Putative tRNA-like genes encoded by  $\gamma$ HV68

tRNA no.	Genome location (bp)	Putative tRNA type	Putative anticodon
t.1	127–200	?	?
t.2	488–561	?	?
t.3	894–967	Val	AAC
t.4	1182–1254	Met	CAT
t.5	1588–1659	Thr	AGT
t.6	3676–3748	?	?
t.7	4946–5029	?	?
t.8	5384–5457	?	?

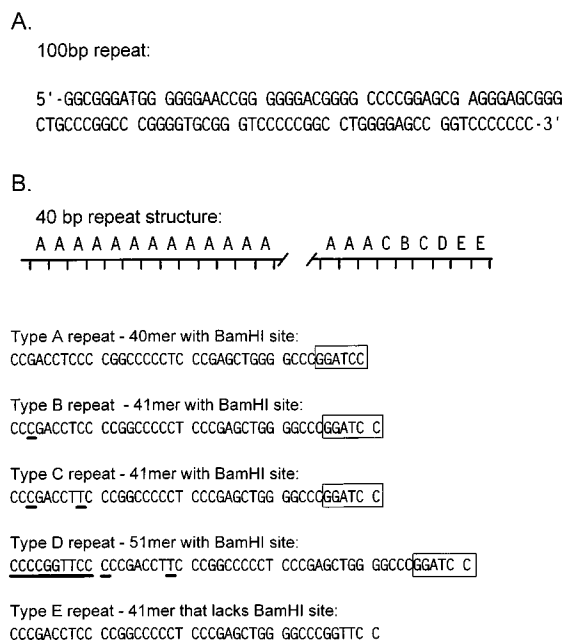


FIG. 2. Sequence and structure of the internal repeats present in the  $\gamma$ HV68 genome. (A) Sequence of the 100-bp repeat (only the top strand is shown). Analysis of the 100-bp repeat region indicates that the repeat is made up of 21 intact copies of the repeat and a partial copy of the repeat at the right-hand end which is lacking the last 10 bp of the repeat. (B) Organization and sequence of the 40-bp repeat. The repeat is estimated to contain 27 complete copies of the A repeat linked to several degenerate forms of the repeat located at the right-hand end of the repeat (type B to E repeats), as illustrated. The sequences of each type of repeat is shown below the schematic diagram of the repeat structure. Residues which differ from the type A repeat are underlined, and the presence of a *Bam*HI site is indicated by the open rectangle.

**Analysis of repeats in the  $\gamma$ HV68 genome.** In addition to the terminal repeat, the  $\gamma$ HV68 genome contains two internal repeats (Fig. 2), a 40-bp repeat located between bp 26778 and 28191 in the genome and a 100-bp repeat located between bp 98981 and 101170 in the genome. Both repeats are very G+C rich; the 100-bp repeat is 86% G+C, while the 40-bp repeat is 83% G+C.

(i) **The 100-bp repeat.** The region of the 100-bp repeat (Fig. 2A) was constructed by combining the following data: (i) sequences of multiple M13 clones spanning the left and right junctions between the 100-bp repeats and unique sequence, (ii) sequencing a series of exonuclease III-generated nested deletions spanning the 100-bp repeat region (see Materials and Methods), and (iii) estimation of the size of the repeat region (cloned from genomic DNA) by restriction endonuclease digestion. These multiple pieces of data were required because the highly repetitive nature and size of the region prevented us from obtaining unambiguous sequence from M13 clones alone. This was due to our inability to unambiguously anchor sequences initiating within the 100-bp repeat in the contig. The 100-bp repeat is predicted to span from bp 98981 to 101170 and to contain 21 complete copies of the 100-mer repeat shown in Fig. 2A and a 90-bp partial repeat at the right end of the 100-bp repeat region.

(ii) **The 40-bp repeat.** The region of the 40-bp repeat was constructed by using the following data: (i) sequences of multiple M13 clones spanning the left and right borders between the 40-bp repeats and unique sequence and (ii) estimation of the size of the repeat region (derived from genomic DNA) by restriction endonuclease digestion analyses. We failed to stably

clone the 40-bp repeat region; numerous clones were recovered, all of which had spontaneously deleted portions of the repeat. M13 clones spanning the left junction between unique sequence and the repeat region entered into a series of 40-bp repeats each containing a *Bam*HI site (type A repeats [Fig. 2B]). The first A repeat at the left-hand end is a partial repeat containing the last 27 bp of the type A repeat. M13 clones spanning the right junction between unique sequence and the repeat region spanned several repeats that were similar in structure to the A repeats (B, C, D, and E repeats [Fig. 2B]) prior to entering A repeats. The rightmost two repeats (type E repeats) are 41-mers that lack the internal *Bam*HI site. There is also a slightly longer 51-bp variant (type D repeat) which contains the internal *Bam*HI site and two other 41-mer variants (type B and C repeats) which also contain the internal *Bam*HI site. We concluded that the majority of the repeat is composed of an estimated 27 copies of the 40-mer A repeat (Fig. 2B) based on the fact that M13 clones from both right and left junctions between unique sequence and repeat sequence end with 40-bp repeat A sequences. It is possible that other sequences that could not be detected by our analysis are present centrally within the 40-bp repeat sequence. It is perhaps notable that all variant repeats which were detected map to the right end of the repeat, suggesting that maintaining the integrity of the central and left-hand portions of this repeat region may be functionally important.

(iii) **The terminal repeat.** The terminal repeat was sequenced multiple times from M13 clones spanning the 5' and 3' junctions between unique sequence and the terminal repeats. A single copy of the 1,213-bp terminal repeat is attached to the right end of the  $\gamma$ HV68 unique sequence submitted to GenBank. It should be noted that the beginning of the consensus terminal repeat unit was defined by the border between the terminal repeat and nucleotide 1 of the genome. This assignment, based on the sequences of M13 clones spanning the right-hand junction between unique sequence and the terminal repeat, results in a 26-bp portion of the terminal repeat at the right-hand end of the unique region of the  $\gamma$ HV68 genome before the first intact terminal repeat. As discussed above, the terminal repeat encodes a putative polypeptide (M14) which would be initiated from one of two potential methionine initiation codons present in this very G+C rich sequence, thus generating an ORF which is represented many times in the intact viral genome. In addition, two ORFs (M12 and M13) begin outside the terminal repeat but extend into the terminal repeat. We also evaluated the left end of the genome attached to the terminal repeat but found no ORFs meeting our criteria (see above). The significance of these putative ORFs that include G+C-rich terminal repeat sequences is not known.

**Comparison of genome organization among gammaherpesviruses.** The genomes of herpesviruses tend to contain blocks of conserved genes interspersed with blocks of genes specific to a viral family or a specific virus (17). In agreement with the close structural homology between the  $\gamma$ HV68 genome and the genomes of KSHV, HVS, and EBV, phylogenetic analyses of the predicated DNA polymerase and major capsid proteins supported the assignment of  $\gamma$ HV68 as a gammaherpesvirus (data not shown) (17, 38). To further assess the relationship between  $\gamma$ HV68 and primate gammaherpesviruses, we compared the gene organizations of HVS, KSHV,  $\gamma$ HV68, and EBV genomes. This analysis revealed a strong conservation of specific blocks of genes, separated by genes that appear to be largely virus specific (Fig. 3). None of the EBV latency-associated genes (i.e., the EBNA or LMP genes) appears to be conserved among the gammaherpesviruses. In addition, the trans-

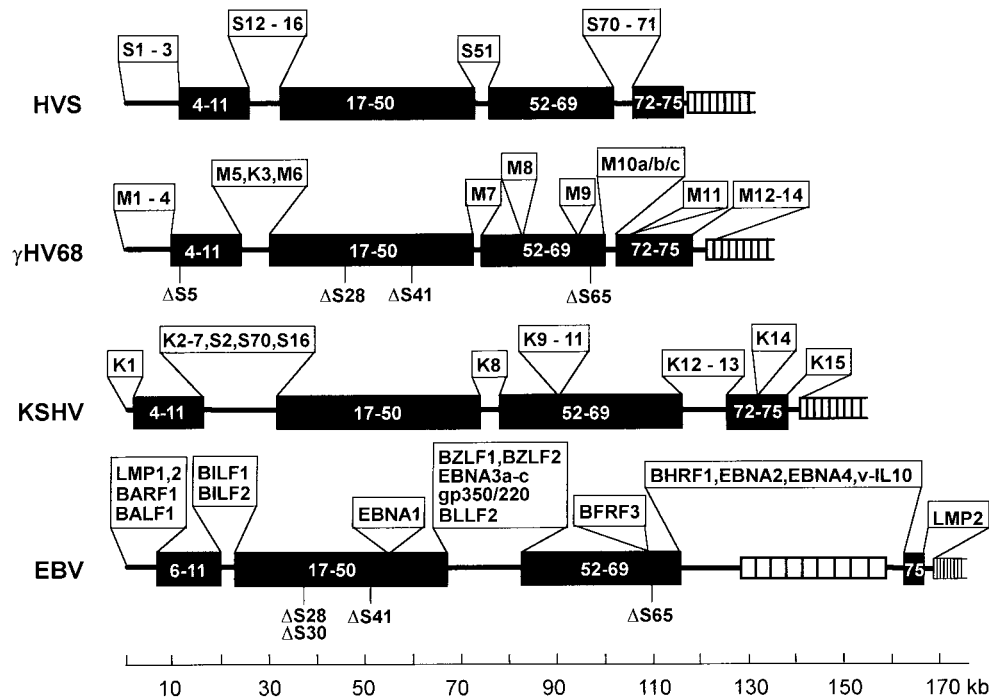


FIG. 3. Comparison of genome organization among gammaherpesviruses. The structures of the indicated viruses were compared to the HVS genome structure. The conserved blocks of genes are indicated in the shaded rectangles, and the numbers correspond to the HVS gene numbers. Genes missing from particular blocks are indicated below each block (specific genes which are missing are indicated with a  $\Delta$ ), while genes inserted within a particular block of genes are indicated above each block. The terminal repeats located at the ends of the gammaherpesvirus genomes are shown only at the right-hand end of the respective genomes. The major internal repeat of EBV is shown near the right-hand end of the genome as a series of connected open rectangles. ORFs designated with an S are largely unique to HVS; ORFs designated with an M are largely unique to  $\gamma$ HV68; ORFs designated with a K are largely unique to KSHV.

formation-associated HVS gene products STP and TIP do not appear to have homologs in the other gammaherpesviruses. This observation raises the possibility that many of the latency- and transformation-associated genes in  $\gamma$ HV68 and KSHV are encoded by virus-specific genes. In addition, it suggests that while functions required for lytic replication of these viruses have generally been well conserved, strategies for latency have diverged significantly. This may reflect both cell-type- and species-specific constraints. Alternatively, it is possible that the ability of gammaherpesviruses to establish a latent infection has independently evolved in each of these viruses. The latter possibility seems unlikely given that the ability to establish a latent infection is a hallmark of all characterized herpesviruses.

**Homologs of cellular or viral genes potentially involved in pathogenesis, latency, or tumor induction.** It is notable that  $\gamma$ HV68 contains homologs of several viral and host genes that may be important for gammaherpesvirus pathogenesis (Fig. 4). Similar to HVS and KSHV,  $\gamma$ HV68 contains an ORF (ORF 4) with significant homology to multiple complement regulatory proteins (3, 42, 61). The presence of four regions within  $\gamma$ HV68 ORF 4 with homology to complement control protein repeats or short consensus repeats results in significant

BLASTP alignments with many complement regulatory proteins (42). Notably,  $\gamma$ HV68 ORF 4 aligns particularly well over the entire length of the predicted protein with murine decay-accelerating factor (DAF) and human membrane cofactor protein (MCP) (Fig. 4A). Both DAF and MCP regulate C3 convertase (although by different mechanisms), suggesting that regulation of C3 convertase is a potential action of ORF 4 of  $\gamma$ HV68. This hypothesis is consistent with studies of the HVS gene 4 product, which inhibits C3-mediated lysis (29).

ORF 72 of  $\gamma$ HV68 is predicted to encode a D-type cyclin. The fact that KSHV, HVS, and  $\gamma$ HV68 encode cyclin homologs (13, 16, 36, 41, 51), combined with the fact that EBV regulates cellular cyclin D expression (62), strongly argues for a conserved role of this gene product in gammaherpesvirus biology. An alignment of the  $\gamma$ HV68 ORF 72 with mouse cyclin D1, KSHV v-cyclin, and HVS v-cyclin is shown in Fig. 4B. The proteins all share conserved residues (e.g., the  $\gamma$ HV68 TWM sequence at position 62 in the alignment) within the cyclin box. A mutagenesis study of this region of the HVS v-cyclin showed that several residues conserved between  $\gamma$ HV68 ORF 72 and the HVS v-cyclin are involved in binding to cyclin-dependent kinase 6 (cdk6) (36). In addition, the

FIG. 4. Alignments of five  $\gamma$ HV68 ORFs with viral or host homologs. All alignments were performed with MegAlign (DNASTAR) and are presented without reediting after the initial alignment was performed. Residues shown in green are chemically related, while red indicates the presence of identical residues among some of the sequences (at some positions both red and green highlighted residues are shown, which indicates that all of the colored residues are chemically related and some of them are identical). Blue denotes those residues which are identical in all the aligned protein sequences. For each of the alignments described below, the number in parentheses is the GenBank or SWISS-PROT accession number (GB or SP acc.). All HVS, KSHV, and EBV sequences were derived from the original publications (3, 6, 61). (A) Alignment of mouse DAF (GB acc. L41366), human MCP (SP acc. P15529), and  $\gamma$ HV68 ORF 4. (B) Alignment of murine cyclin D1 (GB acc. M64403),  $\gamma$ HV68 ORF 72, KSHV gene 72, and HVS gene 72. (C) Alignment of mouse *bcl-2* (GB acc. M16506),  $\gamma$ HV68 ORF M11, and EBV BHRF1. (D) Alignment of  $\gamma$ HV68 ORF M1, rabbitpox *SPI-1* (SP acc. P42928), and cowpox *crmA* (GB acc. M14217). (E) Alignment of the mouse IL-8 receptor (SP acc. P35343),  $\gamma$ HV68 ORF 74, KSHV gene 74, and HVS gene 74.





KSHV v-cyclin associates with cdk6 and to a lesser extent with cdk4 (41). These data suggest that the  $\gamma$ HV68 v-cyclin may also interact with specific cyclin-dependent kinases. Interestingly, we have not found a clear homolog of the LxCxE motif found to be important for retinoblastoma protein binding to cyclin D (22, 27). Notably, this motif is also lacking in the HVS and KSHV v-cyclins, raising the possibility that the v-cyclins do not interact with the retinoblastoma protein. Alternatively, it is possible that additional exons are spliced to the viral ORF 72 to form a protein containing the LxCxE motif (or other sequences). The fact that KSHV and HVS v-cyclins are expressed in Kaposi's sarcoma tissues (13) and transformed cell lines (36), respectively, raises the possibility that the  $\gamma$ HV68 v-cyclin is involved in oncogenesis or latency. However, a role in lytic infection has not been ruled out by studies to date of the HVS and KSHV v-cyclins.

$\gamma$ HV68 ORF M11 has weak overall homology to *bcl-2* family members and encodes a protein with 24% amino acid identity with the EBV BHRF1 gene product (Fig. 4C). The latter has been shown to inhibit apoptosis in several systems (33, 69). Similarly, the KSHV *bcl-2* homolog (gene 16) inhibits apoptosis (14). We designated this ORF M11 rather than calling it either ORF 16 (as a homolog of the HVS and KSHV gene 16) or BHRF1, since the level of homology is weak enough that the proteins could have distinct functions (Fig. 4C). It is clear from a survey of the known viral Bcl-2 homologs that there is only limited sequence conservation between these proteins and the cellular counterparts. Thus, it is perhaps not surprising that the viral *bcl-2* genes may have also diverged significantly from each other. The greatest local homology between Bcl-2 family members and the  $\gamma$ HV68 M11 ORF product is within the box 1 motif involved in dimerization of Bcl-2 family members (data not shown). This raises the possibility that  $\gamma$ HV68 M11 functions by interacting with itself or host Bcl-2 family members, although this type of association may not be essential for the KSHV gene 16 product to inhibit apoptosis (14).

It is notable that the  $\gamma$ HV68 M11 ORF (potential *bcl-2* homolog) is located in the same position in the genome as the EBV *bcl-2* homolog (BHRF1 gene). Thus, EBV and  $\gamma$ HV68 have a common arrangement of their *bcl-2* homologs. Notably, while the KSHV *bcl-2* homolog (gene 16) is located in the same place as the HVS gene 16, the KSHV *bcl-2* homolog is adjacent to an HVS gene 70 homolog (Fig. 3). This finding suggests that in an ancestral gammaherpesvirus, the *bcl-2* homolog was located near the right-hand end of the unique region (near gene 70). Rearrangement of this ancestral genome could have moved the *bcl-2* homolog to its current location in the HVS and KSHV genomes. In the case of KSHV, this speculative rearrangement included gene 70. This argues for placement of the ancestral *bcl-2* homolog in the same position as the  $\gamma$ HV68 M11 and EBV BHRF1 genes.

$\gamma$ HV68 also contains an ORF (M1) which is predicted to encode a protein homologous to several poxvirus serpins (Fig. 4D). This ORF product is the first reported serpin homolog encoded by a herpesvirus. The fact that similar ORFs have not been found in HVS, KSHV, and EBV suggests that this ORF may provide a virus- or host-specific function unique to  $\gamma$ HV68. Significant homology was found between  $\gamma$ HV68 M1 and the *SPI-1* genes of rabbitpox, cowpox, vaccinia, and variola viruses (Fig. 4D) (4). Interestingly, the poxvirus *SPI-1* gene can regulate host cell range by altering apoptosis (9). There is also significant homology between the  $\gamma$ HV68 M1 ORF and *crmA* (Fig. 4D) (59). This raises the possibility that the  $\gamma$ HV68 serpin may alter the function of interleukin 1 (IL-1)-converting enzyme-like proteases. It is notable that poxvirus serpins have been implicated in a broad range of processes in addition to

regulating apoptosis, including regulation of inflammatory responses and altering arachidonate (4, 9, 18, 44, 52, 53, 56, 59, 72). The specific role of viral serpins may depend on the enzyme(s) targeted (43) and the host pathogenesis model evaluated (71).

$\gamma$ HV68 contains an ORF (ORF 74) homologous to genes encoding G-protein-coupled receptors (GCRs). Similar to gene 74 in both HVS and KSHV, the  $\gamma$ HV68 ORF 74 is most homologous to the IL-8 receptor (Fig. 4E) (1, 3, 5, 51, 61). Structure analysis demonstrates seven potential transmembrane domains (not shown). The HVS ORF 74 product has been shown to be a functional IL-8 receptor in transfection experiments (1). This finding suggests the possibility that host cytokines signaling through the viral GCR could alter the virus life cycle. In contrast, the KSHV gene 74 product is a constitutively active GCR that can bind both  $\alpha$  and  $\beta$  chemokines and can provide a signal for cell growth (5). As the KSHV gene has been demonstrated to be expressed in tumors (13), it is possible that these receptors play a role in tumor induction or maintenance of tumor growth. However, a role in latency or lytic infection is also possible.

$\gamma$ HV68 contains an ORF (K3) homologous to ORFs K3 and K5 of KSHV as well as the bovine herpesvirus 4 major immediate-early (BHV4 IE1) transcript (61, 75). The homology between KSHV K3, KSHV K5,  $\gamma$ HV68 K3, and BHV4 IE1 is local and is marked by complete conservation of a motif CWIC-(10/11x)-CxXXXXXXXXHxxCxxxWxxxxSxxxxCxxCxxxY. Interestingly, this motif is also present in a hypothetical swinepox virus protein (C7; SWISS-PROT accession no. P32225) and is well conserved in the amino-terminal portion of the *Caenorhabditis elegans* F58E6.1 protein (EMBL accession no. Z70754). This is an additional example (together with the serpin homolog described above) of conservation between poxvirus and herpesvirus genes. The importance of this motif is not known, but it may represent a part of a zinc finger motif. Conservation of this motif across multiple viruses and *C. elegans* suggests an important role in the function of these proteins.

**Summary.** The complete nucleotide sequence of the  $\gamma$ HV68 genome demonstrates that this murine herpesvirus is a gammaherpesvirus with similarities to HVS, KSHV, and EBV. The presence of cyclin, GCR, serpin, Bcl-2, and DAF/MCP homologs provides an opportunity to evaluate the roles of the genes encoding these proteins in viral pathogenesis. In addition, the identification of a number of apparently virus-specific ORFs in the  $\gamma$ HV68 genome offers the opportunity to assess their contribution to  $\gamma$ HV68 pathogenesis, latency, and tumor induction in a tractable small-animal model.

#### ACKNOWLEDGMENTS

This work was partially supported by grants to H.W.V. from the NIH (AI39615), the Mallinckrodt Foundation, and the Council for Tobacco Research and by American Cancer Society Junior Faculty Research Award JFRA-525. K.E.W. was supported by NIH grant K08 AI01279-01AI. S.H.S. was supported by NIH grants CA43143, CA52004, and CA58524.

We thank Dave O'Brien and Alicia Gibson for their work producing the  $\gamma$ HV68 sequence.

#### REFERENCES

- Ahuja, S. K., and P. M. Murphy. 1993. Molecular piracy of mammalian interleukin-8 receptor type B by herpesvirus saimiri. *J. Biol. Chem.* **268**: 20691-20694.
- Albrecht, J.-C., and B. Fleckenstein. 1992. Nucleotide sequence of HSUR6 and HSUR7, two small RNAs of herpesvirus saimiri. *Nucleic Acids Res.* **20**:1810.
- Albrecht, J.-C., J. Nicholas, D. Biller, K. R. Cameron, B. Biesinger, C. Newman, S. Wittmann, M. A. Craxton, H. Coleman, B. Fleckenstein, and R. W. Honess. 1992. Primary structure of the herpesvirus saimiri genome. *J. Virol.* **66**:5047-5058.

4. Ali, A. N., P. C. Turner, M. A. Brooks, and R. W. Moyer. 1994. The SPI-1 gene of rabbitpox virus determines host range and is required for hemorrhagic pox formation. *Virology* **202**:305–314.
5. Arvanitakis, L., E. Geras-Raaka, A. Varma, M. C. Gershengorn, and E. Cesarman. 1997. Human herpesvirus KSHV encodes a constitutively active G-protein-coupled receptor linked to cell proliferation. *Nature* **385**:347–350.
6. Baer, R., A. T. Bankier, M. D. Biggin, P. L. Deininger, P. J. Farrell, T. J. Gibson, G. Hatfull, G. S. Hudson, S. C. Satchwell, C. Seguin, P. S. Tuffnell, and B. G. Barrell. 1984. DNA sequence and expression of the B95-8 Epstein-Barr virus genome. *Nature* **310**:207–209.
7. Blaskovic, D., M. Stancekova, J. Svobodova, and J. Mistrikova. 1980. Isolation of five strains of herpesviruses from two species of free living small rodents. *Acta Virol.* **24**:468.
8. Blaskovic, D., D. Stanekova, and J. Rajcani. 1984. Experimental pathogenesis of murine herpesvirus in newborn mice. *Acta Virol.* **28**:225–231.
9. Brooks, M. A., A. N. Ali, P. C. Turner, and R. W. Moyer. 1995. A rabbitpox virus serpin gene controls host range by inhibiting apoptosis in restrictive cells. *J. Virol.* **69**:7688–7698.
10. Cardin, R. D., J. W. Brooks, S. R. Sarawar, and P. C. Doherty. 1996. Progressive loss of CD8+ T cell-mediated control of a gamma-herpesvirus in the absence of CD4+ T cells. *J. Exp. Med.* **184**:863–871.
11. Cavanaugh, V. J., R. M. Stenberg, T. L. Staley, H. W. Virgin, M. R. MacDonald, S. Paetzold, H. E. Farrell, W. D. Rawlinson, and A. E. Campbell. 1996. Murine cytomegalovirus with a deletion spanning *HindIII*-J and -I displays altered cell and tissue tropism. *J. Virol.* **70**:1365–1374.
12. Cesarman, E., Y. Chang, P. S. Moore, J. W. Said, and D. M. Knowles. 1995. Kaposi's sarcoma-associated herpesvirus-like DNA sequences in AIDS-related body-cavity-based lymphomas. *N. Engl. J. Med.* **332**:1186–1191.
13. Cesarman, E., R. G. Nador, F. Bai, R. A. Bohenzky, J. J. Russo, P. S. Moore, Y. Chang, and D. M. Knowles. 1996. Kaposi's sarcoma-associated herpesvirus contains G protein-coupled receptor and cyclin D homologs which are expressed in Kaposi's sarcoma and malignant lymphoma. *J. Virol.* **70**:8218–8223.
14. Chang, E. H.-Y., J. Nicholas, D. S. Bellows, G. S. Hayward, H.-G. Guo, M. S. Reitz, and J. M. Hardwick. 1997. A bcl-2 homolog encoded by Kaposi's sarcoma-associated virus, human herpesvirus 8, inhibits apoptosis but does not heterodimerize with Bax or Bak. *Proc. Natl. Acad. Sci. USA* **94**:690–694.
15. Chang, Y., E. Cesarman, M. S. Pessin, F. Lee, J. Culpepper, D. M. Knowles, and P. S. Moore. 1994. Identification of herpesvirus-like DNA sequences in AIDS-associated Kaposi's sarcoma. *Science* **266**:1865–1869.
16. Chang, Y., P. S. Moore, S. J. Talbot, C. H. Boshoff, T. Zarkowska, D. Godden-Kent, H. Paterson, R. A. Weiss, and S. Mittnacht. 1996. Cyclin encoded by KS herpesvirus. *Nature* **382**:410.
17. Chee, M. S., S. B. Bankier, C. M. Bohni, R. C. Brown, T. Horsnell, C. A. Hitchinson, T. Kouzarides, J. A. Martignetti, E. Preddie, S. C. Satchwell, P. Tomlinson, K. M. Weston, and B. G. Barrell. 1990. Analysis of the protein-coding content of the sequence of human cytomegalovirus strain AD169. *Curr. Top. Microbiol. Immunol.* **154**:125–169.
18. Chua, T. P., C. E. Smith, R. W. Reith, and J. D. Williamson. 1990. Inflammatory responses and the generation of chemoattractant activity in cowpox virus-infected tissues. *Immunology* **69**:202–208.
19. Dear, S., and R. Staden. 1991. A sequencing assembly and editing program for efficient management of large projects. *Nucleic Acids Res.* **19**:3907–3911.
20. Decker, L. L., P. Shankar, G. Khan, R. B. Freeman, B. J. Dezube, J. Lieberman, and D. A. Thorley-Lawson. 1996. The Kaposi's sarcoma-associated herpesvirus (KSHV) is present as an intact latent genome in KS tissue but replicates in the peripheral blood mononuclear cells of KS patients. *J. Exp. Med.* **184**:283–288.
21. Desrosiers, R. C., A. Bakker, J. Kamine, L. A. Falk, R. D. Hunt, and N. W. King. 1985. A region of the herpesvirus saimiri genome required for oncogenicity. *Science* **228**:184–187.
22. Dowdy, S. F., P. W. Hinds, K. Louie, S. I. Reed, A. Arnold, and R. A. Weinberg. 1993. Physical interaction of the retinoblastoma protein with human D cyclins. *Cell* **73**:499–511.
- 22a. Durbin, R. (MRC Laboratory of Molecular Biology, Cambridge, England). Unpublished data.
- 22b. Durbin, R. (MRC Laboratory of Molecular Biology, Cambridge, England) and J. Thierry-Mieg (Centre de Recherche en Biochimie Macromoleculaire, CNRS, Montpellier, France). Unpublished data.
23. Eddy, S. R., and R. Durbin. 1994. RNA sequence analysis using covariance models. *Nucleic Acids Res.* **22**:2079–2088.
24. Efsthathiou, S., Y. M. Ho, S. Hall, C. J. Styles, S. D. Scott, and U. A. Gompels. 1990. Murine herpesvirus 68 is genetically related to the gammaherpesviruses Epstein-Barr virus and herpesvirus saimiri. *J. Gen. Virol.* **71**:1365–1372.
25. Efsthathiou, S., Y. M. Ho, and A. C. Minson. 1990. Cloning and molecular characterization of the murine herpesvirus 68 genome. *J. Gen. Virol.* **71**:1355–1364.
26. Ehtisham, S., N. P. Sunil-Chandra, and A. A. Nash. 1993. Pathogenesis of murine gammaherpesvirus infection in mice deficient in CD4 and CD8 T cells. *J. Virol.* **67**:5247–5252.
27. Ewen, M. E., H. K. Sluss, C. J. Sherr, H. Matsushime, J.-Y. Kato, and D. M. Livingston. 1993. Functional interactions of the retinoblastoma protein with mammalian D-type cyclins. *Cell* **73**:487–497.
28. Fichant, G. A., and C. Burks. 1991. Identifying potential tRNA genes in genomic DNA sequences. *J. Mol. Biol.* **220**:659–671.
29. Fodor, W. L., S. A. Rollins, S. Bianco-Caron, R. P. Rother, E. R. Guilmette, W. V. Burton, J.-C. Albrecht, B. Fleckenstein, and S. P. Squinto. 1995. The complement control protein homolog of herpesvirus saimiri regulates serum complement by inhibiting C3 convertase activity. *J. Virol.* **69**:3889–3892.
30. Fulton, L. L., and R. K. Wilson. 1994. Variations on cycle sequencing. *BioTechniques* **17**:298–301.
31. Geck, P., S. A. Whitaker, M. M. Medveczky, T. J. Last, and P. G. Medveczky. 1994. Small RNA expression from the oncogenic region of a highly oncogenic strain of herpesvirus saimiri. *Virus Genes* **8**:25–34.
32. Geck, P., S. A. Whitaker, M. M. Medveczky, and P. G. Medveczky. 1990. Expression of collagen like sequences by a tumor virus, herpesvirus saimiri. *J. Virol.* **64**:3509–3515.
- 32a. Green, P. (University of Washington, Seattle). Unpublished data.
33. Henderson, S., D. Huen, M. Rowe, C. Dawson, G. Johnson, and A. Rickinson. 1993. Epstein-Barr virus-coded BHRF1 protein, a viral homologue of Bcl-2, protects human B cells from programmed cell death. *Proc. Natl. Acad. Sci. USA* **90**:8479–8483.
- 33a. Hillier, L. (The Genome Sequencing Center, Department of Genetics, Washington University School of Medicine). Unpublished data.
34. Huang, Y. Q., J. J. Li, M. H. Kaplan, B. Poiesz, E. Katabira, W. C. Zhang, D. Feiner, and A. E. Friedman-Kien. 1995. Human herpesvirus-like nucleic acid in various forms of Kaposi's sarcoma. *Lancet* **345**:759–761.
35. Ju, J., C. Ruan, C. W. Fuller, A. N. Glazer, and R. A. Mathies. 1995. Fluorescence energy transfer dye-labelled primers for DNA sequencing and analysis. *Proc. Natl. Acad. Sci. USA* **92**:4347–4351.
36. Jung, J. U., M. Stager, and R. C. Desrosiers. 1994. Virus-encoded cyclin. *Mol. Cell. Biol.* **14**:7235–7244.
37. Jung, J. U., J. J. Trimble, N. W. King, B. Biesinger, B. W. Fleckenstein, and R. C. Desrosiers. 1991. Identification of transforming genes of subgroup A and C strains of herpesvirus saimiri. *Proc. Natl. Acad. Sci. USA* **88**:7051–7055.
38. Karlin, S., E. S. Mocarski, and G. A. Schachtel. 1994. Molecular evolution of herpesviruses: genomic and protein sequence comparisons. *J. Virol.* **68**:1886–1902.
39. Kieff, E. 1996. Epstein-Barr virus and its replication, p. 2343–2396. *In* B. Fields, D. Knipe, and P. Howley (ed.), *Fields' virology*. Lippincott-Raven, Philadelphia, Pa.
40. Li, J. J., Y. Q. Huang, C. J. Cockerell, and A. E. Friedman-Kien. 1996. Localization of human herpes-like virus type 8 in vascular endothelial cells and perivascular spindle-shaped cells of Kaposi's sarcoma lesions by in situ hybridization. *Am. J. Pathol.* **148**:1741–1748.
41. Li, M., H. Lee, D.-W. Yoon, J.-C. Albrecht, B. Fleckenstein, F. Neipel, and J. U. Jung. 1997. Kaposi's sarcoma-associated herpesvirus encodes a functional cyclin. *J. Virol.* **71**:1984–1991.
42. Liszewski, M. K., T. C. Farries, D. M. Lublin, I. Rooney, and J. P. Atkinson. 1996. Control of the complement system. *Adv. Immunol.* **61**:201–283.
43. Lomas, D. A., D. L. Evans, C. Upton, G. McFadden, and R. W. Carrell. 1992. Inhibition of plasmin, urokinase, tissue plasminogen activator, and CIs by a myxoma virus serine proteinase inhibitor. *J. Biol. Chem.* **268**:516–521.
- 43a. Lowe, T., and S. R. Eddy (The Genome Sequencing Center, Department of Genetics, Washington University School of Medicine). Unpublished data.
44. Macen, J. L., C. Upton, N. Nation, and G. McFadden. 1993. SERP-I, a serine proteinase inhibitor encoded by myxoma virus, is a secreted glycoprotein that interferes with inflammation. *Virology* **195**:348–363.
45. Mardis, E. R. 1994. High-throughput detergent extraction of M13 clones for fluorescent DNA sequencing. *Nucleic Acids Res.* **22**:2173–2175.
- 45a. Marth, G., and L. Hillier (The Genome Sequencing Center, Department of Genetics, Washington University School of Medicine). unpublished
46. Medveczky, M., P. Geck, J. L. Sullivan, D. Serbousek, J. Y. Djeu, and P. G. Medveczky. 1993. IL-2 independent growth and cytotoxicity of herpesvirus saimiri-infected human CD8 cells and involvement of two open reading frame sequences of the virus. *Virology* **196**:402–412.
47. Medveczky, M. M., P. Geck, R. Vassallo, and P. G. Medveczky. 1993. Expression of the collagen-like putative oncoprotein of herpesvirus saimiri in transformed T cells. *Virus Genes* **7**:349–365.
48. Mistrikova, J., and D. Blaskovic. 1985. Ecology of the murine alphaherpesvirus and its isolation from lungs of rodents in cell culture. *Acta Virol.* **29**:312–317.
49. Moore, P. S., and Y. Chang. 1995. Detection of herpesvirus-like DNA sequences in Kaposi's sarcoma in patients with and without HIV infection. *N. Engl. J. Med.* **332**:1181–1185.
50. Murthy, S. C. S., J. J. Trimble, and R. C. Desrosiers. 1989. Deletion mutants of herpesvirus saimiri define an open reading frame necessary for transformation. *J. Virol.* **63**:3307–3314.
51. Nicholas, J., K. R. Cameron, and R. W. Honess. 1992. Herpesvirus saimiri encodes homologs of G protein-coupled receptors and cyclins. *Nature* **355**:362–365.
52. Palumbo, G. J., W. C. Glasgow, and R. M. L. Buller. 1997. Poxvirus-induced

- alteration of arachidonate metabolism. *Proc. Natl. Acad. Sci. USA* **90**:2020–2024.
53. **Palumbo, G. J., D. J. Pickup, T. N. Fredrickson, J. McIntyre, and R. M. Buller.** 1989. Inhibition of inflammatory response is mediated by a 38-kDa protein of cowpoxvirus. *Virology* **172**:262–273.
  54. **Pavesi, A., F. Conterio, A. Bolchi, G. Dieci, and S. Ottonello.** 1994. Identification of new eukaryotic tRNA genes in genomic DNA databases by using a multistep weight matrix analysis of transcription control regions. *Nucleic Acids Res.* **22**:1247–1256.
  55. **Pepper, S. D., J. P. Stewart, J. R. Arrand, and M. Mackett.** 1996. Murine gammaherpesvirus-68 encodes homologues of thymidine kinase and glycoprotein H: sequence, expression, and characterization of pyrimidine kinase activity. *Virology* **219**:475–479.
  56. **Pickup, D. J., B. S. Ink, W. Hu, C. A. Ray, and W. K. Joklik.** 1986. Hemorrhage in lesions caused by cowpox virus is induced by a viral protein that is related to plasma protein inhibitors of serine proteases. *Proc. Natl. Acad. Sci. USA* **83**:7698–7702.
  57. **Pollock, J. L., and H. W. Virgin.** 1995. Latency, without persistence, of murine cytomegalovirus in spleen and kidney. *J. Virol.* **69**:1762–1768.
  58. **Rajcani, J., D. Blaskovic, J. Svobodova, F. Ciampor, D. Huckova, and D. Stanekova.** 1985. Pathogenesis of acute and persistent murine herpesvirus infection in mice. *Acta Virol.* **29**:51–60.
  59. **Ray, C. A., R. A. Black, S. R. Kronheim, T. A. Greenstreet, P. R. Sleath, G. S. Salvesen, and D. J. Pickup.** 1992. Viral inhibition of inflammation: cowpox virus encodes an inhibitor of the interleukin-1-beta converting enzyme. *Cell* **69**:597–604.
  60. **Rickinson, A. B., and E. Kieff.** 1996. Epstein-Barr virus, p. 2397–2446. *In* B. N. Fields, D. M. Knipe, and P. M. Howley (ed.), *Virology*. Lippincott-Raven, Philadelphia, Pa.
  61. **Russo, J. J., R. A. Bohenzky, M.-C. Chien, J. Chen, M. Yan, D. Maddalena, J. P. Parry, D. Peruzzi, I. S. Edelman, Y. Chang, and P. S. Moore.** 1996. Nucleotide sequence of the Kaposi sarcoma-associated herpesvirus (HHV8). *Proc. Natl. Acad. Sci. USA* **93**:14862–14867.
  62. **Sinclair, A. J., I. Palmero, A. Holder, G. Peters, and P. J. Farrell.** 1995. Expression of cyclin D2 in Epstein-Barr virus positive Burkitt's lymphoma cell lines is related to methylation status of the gene. *J. Virol.* **69**:1292–1295.
  63. **Soulier, J., L. Grollet, E. Oksenhendler, P. Cacoub, D. Cazals-Hatem, P. Babinet, M.-F. d'Agay, J.-P. Clauvel, M. Raphael, L. Degos, and F. Signaux.** 1995. Kaposi's sarcoma-associated herpesvirus-like DNA sequences in multicentric Castlemann's disease. *Blood* **86**:1276–1280.
  64. **Stewart, J. P., N. J. Janjua, S. D. Pepper, G. Bennion, M. Mackett, T. Allen, A. A. Nash, and J. R. Arrand.** 1996. Identification and characterization of murine gammaherpesvirus 68 gp150: a virion membrane glycoprotein. *J. Virol.* **70**:3528–3535.
  65. **Stewart, J. P., N. J. Janjua, N. P. Sunil-Chandra, A. A. Nash, and J. R. Arrand.** 1994. Characterization of murine gammaherpesvirus 68 glycoprotein B (gB) homologue: similarity to Epstein-Barr virus gB (gp110). *J. Virol.* **68**:6496–6504.
  66. **Sunil-Chandra, N. P., J. Arno, J. Fazakerley, and A. A. Nash.** 1994. Lymphoproliferative disease in mice infected with murine gammaherpesvirus 68. *Am. J. Pathol.* **145**:818–826.
  67. **Sunil-Chandra, N. P., S. Efstathiou, J. Arno, and A. A. Nash.** 1992. Virological and pathological features of mice infected with murine gammaherpesvirus 68. *J. Gen. Virol.* **73**:2347–2356.
  68. **Sunil-Chandra, N. P., S. Efstathiou, and A. A. Nash.** 1992. Murine gamma-herpesvirus 68 establishes a latent infection in mouse B lymphocytes in vivo. *J. Gen. Virol.* **73**:3275–3279.
  69. **Tarodi, B., T. Subramanian, and G. Chinnadurai.** 1994. Epstein-Barr virus BHRF1 protein protects against cell death induced by DNA-damaging agents and heterologous viral infection. *Virology* **201**:404–407.
  70. **Telford, E. A. R., M. S. Watson, H. C. Aird, J. Perry, and A. J. Davison.** 1995. The DNA sequence of equine herpesvirus 2. *J. Mol. Biol.* **249**:520–528.
  71. **Thompson, J. P., P. C. Turner, A. N. Ali, B. C. Crenshaw, and R. W. Moyer.** 1993. The effects of serpin gene mutations on the distinctive pathobiology of cowpox and rabbitpox virus following intranasal inoculation of Balb/c mice. *Virology* **197**:328–338.
  72. **Upton, C., J. L. Macen, D. S. Wishart, and G. McFadden.** 1990. Myxoma virus and malignant rabbit fibroma virus encode a serpin-like protein important for virus virulence. *Virology* **179**:618–631.
  73. **Usherwood, E. J., J. P. Stewart, and A. A. Nash.** 1996. Characterization of tumor cell lines derived from murine gammaherpesvirus-68-infected mice. *J. Virol.* **70**:6516–6518.
  74. **Usherwood, E. J., J. P. Stewart, K. Robertson, D. J. Allen, and A. A. Nash.** 1996. Absence of splenic latency in murine gammaherpesvirus 68-infected B cell-deficient mice. *J. Gen. Virol.* **77**:2819–2825.
  75. **Van Santen, V. L.** 1991. Characterization of the bovine herpesvirus 4 major immediate-early transcript. *J. Virol.* **65**:5211–5224.
  76. **Weck, K. E., M. L. Barkon, L. I. Yoo, S. H. Speck, and H. W. Virgin.** 1996. Mature B cells are required for acute splenic infection, but not for establishment of latency, by murine gammaherpesvirus 68. *J. Virol.* **70**:6775–6780.
  77. **Wilson, R. K., and E. R. Mardis.** Shotgun sequencing. *In* M. Cozza (ed.), *Genomics: a laboratory manual*, in press. Cold Spring Harbor Laboratory Press, Cold Spring Harbor, N.Y.